Evolutionary computing to determine the skin friction capacity of piles embedded in clay and evaluation of the available analytical methods

Alzabeebee, Saif; Chapman, David

DOI:
10.1016/j.trgeo.2020.100372

Evolutionary computing to determine the skin friction capacity of piles embedded in clay and evaluation of the available analytical methods

Saif Alzabeebee, BSc (Hons), MSc (Hons), PhD, GMICE

Geotechnical Engineer, Amey Consulting, International Design hub, The Colmore Building, Birmingham, United Kingdom, B4 6AT

E-mail: Saif.Alzabeebee@gmail.com; Saif.Alzabeebee@amey.co.uk

David N. Chapman, BSc (Hons), DIS, PhD, CEng, MICE, FHEA

Professor of Geotechnical and Underground Engineering, School of Engineering, University of Birmingham, Edgbaston, Birmingham, United Kingdom, B15 2TT

E-mail: D.N.Chapman@bham.ac.uk

Abstract

Deep foundations are very important elements in the routine design of railways and bridges when the loads applied due to these important structures are higher than the bearing capacity of the soil. However, the methods currently available to calculate the bearing capacity of driven piles embedded in clay have been developed based on empirical factors derived from limited tests. Hence, further assessment of these methods and the development of new methods are urgently required. This paper discusses the development of a new robust model to calculate the skin friction capacity of driven piles using the multi-objective evolutionary polynomial regression (MOGA-EPR) analysis. The paper also evaluates the accuracy of the available analytical methods. Real field results of skin friction capacity of driven piles have been used to achieve the objectives of the study. The results showed that the MOGA-EPR predicts the skin friction of driven piles with an excellent accuracy and better than the available analytical methods, with a mean absolute error (MAE), a root mean square error ($RMSE$), mean (μ), a standard deviation (σ), a coefficient of determination (R^2), the variance account for (VAF) and $a20-index$ of 3.4, 4.6, 1.03, 0.24, 0.98, 99, and 0.75, respectively, for the training data, and 4.2, 5.3, 1.12, 0.15, 0.91, 97 and 0.77, respectively, for testing data. In addition, a novel model to predict the skin friction capacity of driven piles has been proposed based on the MOGA-EPR analysis and this model can be used by engineers and researcher with confidence. The evaluation of the analytical methods illustrated that the Lambda method accuracy is better than the Alpha and Beta methods as this method scored a less mean error (MAE = 7.8 and $RMSE$ = 12.5), a less standard deviation (σ = 0.21), a higher coefficient of determination (R^2 = 0.91), higher value for the variance account for (VAF=89) compared with the other analytical methods. In addition, the Beta method scored lowest compared with the other analytical methods with MAE, $RMSE$, μ, σ, R^2, VAF and $a20-index$ of 17.2, 28.0, 1.07, 1.00, 0.55, 40 and 0.37, respectively. The findings of this study will help to achieve robust calculations of pile capacity and reduce uncertainty associated with the choice of the analytical method used in the design of driven piles in clay.

Keywords: Evolutionary polynomial regression analysis; skin friction; driven piles; analytical methods

Highlights:

- A novel mathematical model has been proposed to predict the skin friction capacity of driven piles embedded in clay.
- The Lambda method produced the lowest error and highest coefficient of determination compared with the other analytical methods.
- The Beta method scored lowest in the assessment of the current analytical methods.

1. Introduction

Deep foundations are very important elements in the design of offshore structures, high-rise buildings, railways and bridges when the loads applied due to these important structures are higher than the bearing capacity of the soil (Li et al., 2019). The urgent demand for the expansion of such heavy structures has been the main reason for more reliable and robust design methods to accurately predict the bearing capacity of deep foundations as this is the main factor controlling the design of deep foundations (Doherty and Gavin, 2011; Alkroosh et al., 2015). The main issue is that the design methods used to predict the bearing capacity of deep foundations have been developed based on factors derived from limited tests (Doherty and Gavin, 2011). Therefore, the accuracy of these design methods requires further assessment and testing. In addition, and due to the complexity of the pile behaviour and the limited tests used to develop the design methods, many previous studies have attempted to use data driven methods to predict the bearing capacity and settlement of deep foundations (Singh and Walia, 2017; Shahin, 2016). These previous studies are summarized in Table 1, the summary includes the data driven method/s each study considered, the input parameters, the output of the data driven method/s and the number of data points used.

In addition to Table 1, there are several studies that have been conducted on the skin friction capacity of piles due to the importance of skin friction in practice as most of the piles are designed to allow very small settlement. The acceptance of a very small settlement in practice means that the routine design of these piles is based on the skin friction, as the end bearing capacity requires a settlement equal to or more than 10% of the diameter of the pile and such settlement is not acceptable in practice. Most of the past studies on the skin friction capacity have focused on the use of data driven methods to predict pile capacity, while there is very limited work concerned with the evaluation of the accuracy of the current analytical methods.

Goh (1995) used artificial neural networks (ANN) to predict the skin friction capacity of driven piles embedded in clay and found that the ANN achieved good prediction of the skin friction, where the coefficient of correlation (R) ranged between 0.86 to 0.99 for the training data (the data used in the development of the ANN model) and 0.94 to 0.96 for the testing data. Goh (1995) also found that ANN predicted the skin friction capacity with an accuracy better than the Alpha and Beta methods (Alpha and Beta methods are analytical methods developed to predict the skin friction capacity of pile embedded in cohesive soils and will be discussed in the next section), where the R for the Alpha and Beta methods was equal to 0.98 and 0.73 for the training data, and 0.89 and 0.70 for the testing data. Cherubini and Vessia (2007) evaluated the accuracy of the Alpha method in predicting the skin friction capacity of bored piles embedded in clay.

Samui (2008, 2011) and Prayogo (2018) used a support vector machine (SVM) approach to predict the skin friction capacity of piles embedded in clay and also found that SVM provided good prediction of the skin friction capacity as the SVM produced low root mean square error values (which ranged between 4.4 to 13.9), low mean absolute error values (which ranged between 3.2 to 9.4), and high R values (which ranged between 0.93 to 0.99). Suman et al. (2016) tested the capabilities of multivariate adaptive regression splines (MARS) and functional networks (FN) to predict the skin friction of driven piles embedded in clay. Suman et al. (2016) found that these methods predicted the skin friction capacity with an accuracy better than the ANN, SVM, Alpha and Beta methods, as these methods scored lower mean absolute error values and lower root mean square error values.

Moayedi and Hayati (2018b) developed design charts and a mathematical model to predict the skin friction capacity of driven piles embedded in clay. The design chart was developed based on ANN and the mathematical model was developed based on genetic programing (GP). Samui (2019) used Gaussian Process Regression (GPR) and Minimax Probability Machine Regression (MPMR) to predict the skin friction of driven piles embedded in clay and found that these methods estimated the skin friction capacity better than the ANN. The calculated mean absolute error was equal to 3.2, 2.0 and 2.0 for the ANN, GPR and MPMR, respectively. In addition, the calculated mean root square error for the aforementioned methods was equal to 5.3, 4 and 4, respectively.

Based on the literature review it is clear that many attempts have been made to predict the skin friction capacity of piles embedded in clay using data driven techniques, i.e. using ANN, SVM, MARS, FN, GP, GPR and MPMR. However, ANN is a black box method as it does not give the relationship between the dependent and the independent variables (Faramarzi, 2011); hence, such a technique does not clearly show the influence of the pile length, pile diameter, undrained shear strength and effective stress on the skin friction capacity. Furthermore, SVM, MARS, FN, GP, GPR and MPMR provide complicated models, which cannot be easily interpreted and used. Also, no study in the literature has evaluated the capabilities of multi-objective evolutionary polynomial regression analysis (MOGA-EPR) in predicting the skin friction capacity of piles, although this method provides robust and simple mathematical models as demonstrated in many studies in the literature (Ahangar-Asr et al., 2014, 2016, 2018; Fiore et al., 2016; Alzabeebee et al., 2018, 2019; Alzabeebee, 2019, 2020). In addition, previous studies evaluated the accuracy of Alpha method in predicting the skin friction capacity of bored piles (Cherubini and Vessia, 2007), and Alpha and Beta methods for the case of driven piles (Goh, 1995; Suman et al., 2016). However, Goh (1995) and Suman et al. (2016) did not mention the method used to calculate the α parameter (which is a factor used in the Alpha method to calculate the skin friction capacity of piles embedded in clay) for the case of driven piles, although more than one approach is available in the literature to calculate the α parameter as will be discussed in the next section. In addition, the previous studies did not evaluate the accuracy of the Lambda method, which is also an analytical method to predict the skin friction capacity of piles embedded in clay. Therefore, this study aims to improve the state-of-the-art with respect to the prediction of the skin friction of driven piles by considering two important objectives:

1- The first objective is to use a very powerful and new data driven method to predict the skin friction capacity of driven piles in clay; the method is the multi-objective evolutionary polynomial regression analysis. The strength of this method over the traditional data driven methods is that it has the ability to provide robust and simpler prediction models (Faramarzi, 2011) as the EPR gives the relationship between the parameters in the form of a simple mathematical expression (Ahangar-Asr et al., 2014, 2016, 2018; Alzabeebee et al., 2018, 2019; Nassr et al., 2018a, b). Having an equation as an outcome of the analysis is required to aid future designs and to make it easy to test this equation further when new data becomes available.
2- The second objective is to assess the current analytical methods which have been developed to predict the skin friction capacity of bored piles embedded in

clay and understand the limitations and the capabilities of these methods, and to compare the prediction capabilities of these methods with the predictions from the multi-objective evolutionary polynomial regression analysis.

The methodology of this research is briefly summarized in Figure 1. More details on the methodology will be discussed in Sections 2, 3, 4 and 5.

Table 1: Summary of previous studies which have used data driven methods to predict pile settlement and capacity

Reference	Data driven method used	Input parameters	Output of the data driven method	Number of load tests
Shahin (2010)	ANN	D_{eq}, L, D_{stem}, D_{base}, $q_{c_{tip}}$, $q_{c_{shaft}}$ and Fs	Qu	80 load tests for driven piles and 94 load tests for bored piles
Alkroosh and Nikraz (2011a)	GEP	D, L, $q_{c_{tip}}$, $q_{c_{shaft}}$ and Fs	Qu	50 load tests for bored piles and 28 load tests for driven pile
Alkroosh and Nikraz (2011b)	ANN	D, L, $q_{c_{tip}}$, $q_{c_{shaft}}$, $\Delta(\frac{S}{D})$, P_i and P_{i+1}	S/D	50 load tests for bored piles and 30 load tests for driven pile
Ismail and Jeng (2011)	ANN	D, L, P_i, E and k_s	S/D	98
Alkroosh and Nikraz (2012)	GEP	D_{eq}, L, $q_{c_{tip}}$, Fs, $q_{c_{shaft}}$ and E	Qu	25

Alkroosh and Nikraz (2014)	GEP	D, L, N_{shaft}, N_{tip}, St and HE	Qu	25
Momeni et al. (2014)	ANN enhanced with genetic algorithm (GA) optimization technique	L, A, St, W, and H	Qu	50
Shahin (2014a)	RNN	D, L, $q_{c_{tip}}$, Fs, f_{R-tip} and $f_{R-shaft}$	S/D	38
Shahin (2014b)	RNN	D, L, $q_{c_{tip}}$, Fs, f_{R-tip} and $f_{R-shaft}$	S/D	23
Milad et al. (2015)	ANN and GEP	c'_{avg}, $ø'_{avg}$, δ, γ', FPN, L and A	Qu	100
Momeni et al. (2015)	ANN	L, St, A, N_{shaft}, and N_{tip}	fs, Qp and Qu	36
Armaghani et al. (2017)	ANN and hybrid PSO-ANN	Ls/Lr, D, L, UCS and N_{av}	Qu	132
Nejad and Jaksa (2017)	ANN	Type of pile test, type of pile, type of installation, L, A, E, O, $q_{c_{tip}}$, $q_{c_{shaft}}$, Fs and P_i	S/D	56
Harandizadeh et al. (2018a)	ANFIS	L, D, $q_{c_{tip}}$ and Fs	Qu	72

Harandizadeh et al. (2018b)	RBFNN, BR, LM and MT	c'_{avg}, $\varnothing'_{avg}$, δ, γ', FPN, L and A	Qu	100
Moayedi and Hayati (2018a)	FFNNs and FTDNNs	D, L, $q_{c_{tip}}$ and $q_{c_{shaft}}$	S/D	50
Moayedi and Armaghani (2018)	ANN optimised with imperialism competitive algorithm	$\varnothing'_{shaft}$, $\varnothing'_{tip}$, σ'_{tip}, L and A	Qu	59
Shaik et al. (2018)	ANN optimised with imperialism competitive algorithm and neuro-fuzzy inference system	$\varnothing'_{shaft}$, $\varnothing'_{tip}$, σ'_{tip}, L and A	Qu	59
Chen et al. (2019)	neuro-genetic, neuro-imperialism, GEP and ANN	L, A, St, W, and H	Qu	50
Harandizadeh et al. (2019)	ANFIS–GMDH–PSO and FPNN–GMDH	L, D, $q_{c_{tip}}$ and Fs	fs and Qu	72

Note: ANN: artificial neural networks, D_{eq}: driven pile shaft equivalent diameter, L: length of the pile, D_{stem}: bored pile stem diameter, D_{base}: bored pile base diameter, $q_{c_{tip}}$: weighted average cone point resistance over pile tip failure zone, q_{shaft}: weighted average cone point resistance along pile shaft, Fs: weighted average cone sleeve friction resistance, Qu: ultimate pile capacity, GEP: Gene expression programming, D: diameter of the pile, $\Delta(\frac{S}{D})$: normalized settlement increment, P_i:

current load state, P_{i+1}: future load state, S/D: pile settlement to pile diameter, E: modulus of elasticity of the pile, k_s: soil stiffness, , N_{shaft}: average number of blows of the standard penetration test along the pile shaft, N_{tip}: number of blows of the standard penetration test at the pile tip, St: pile set, HE: hammer energy, A: cross-section area of the pile, W: hammer weight, H: hammer drop height, RNN: recurrent neural networks, f_{R-tip}: friction ratio at the pile tip, $f_{R-shaft}$: friction ratio along the pile shaft, c'_{avg}: average effective cohesions of the soil along the pile shaft, $ø'_{avg}$: average angle of shearing resistance along the pile shaft and pile tip, δ: pile-soil friction angle, γ': effective unit weight of the soil, FPN: flap number, fs: skin friction capacity of the pile, Qp: end bearing capacity of the pile, PSO-ANN: artificial numeral network enhanced with particle swarm optimization, Ls/Lr: length of soil layer to socket length, UCS: uniaxial compressive strength, N_{av}: average number of blows based on the standard penetration test the pile shaft and pile tip, O: perimeter of the pile in contact with the soil, ANFIS: neuro-fuzzy inference system, RBFNN: radial basis function neural network, BR: feedforward Bayesian regulation learning algorithm, LM: feedforward Levenberg-Marquardt algorithm, MT: model tree algorithm, FFNNs: feed-forward neural networks, FTDNNs: focused time-delay neural networks, $ø'_{shaft}$: average shearing resistance along the pile shaft, $ø'_{tip}$: average shearing resistance at the pile tip, σ'_{tip}: effective stress at the pile tip, ANFIS–GMDH–PSO: neuro-fuzzy inference system and group method of data handling structure optimized by particle swarm optimization algorithm, FPNN–GMDH: fuzzy polynomial neural network type group method of data handling

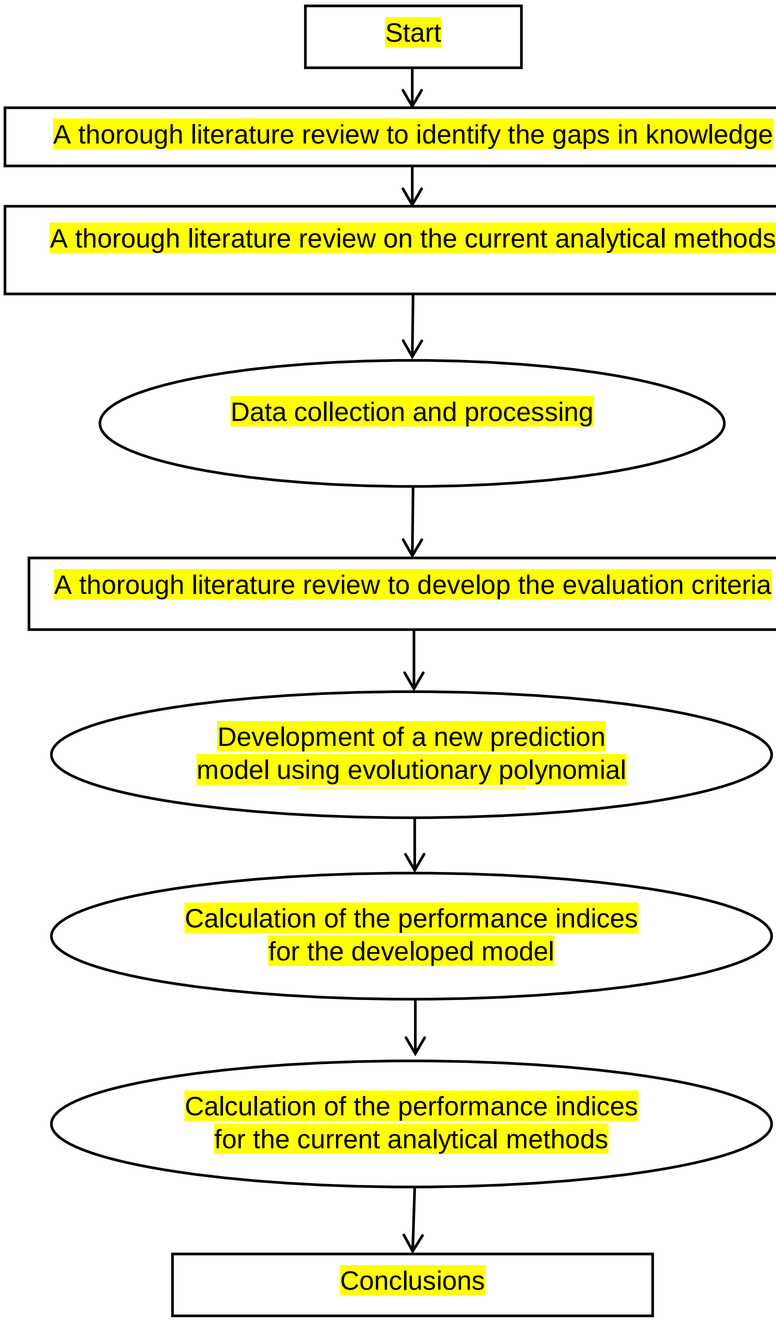

Figure 1: Flow chart of the methodology of this research

2. Current analytical methods

There are currently three analytical methods available in the literature to estimate the skin friction capacity of driven piles embedded in clay (Das, 2011). These methods are:

1- Lambda (λ) method:

This method was proposed by Vijayvergiya and Focht (1972) and is based on the idea that the pile driving into the soil induces passive lateral earth pressure (Das, 2011). The method includes the vertical effective stress (σ'_{ave}) and proposes that the skin friction (fs) of the driven pile can be calculated using Equation 1. The λ factor in Equation 1 depends on the embedment depth of the pile (L) as shown in Figure 2.

$$fs = \lambda(\sigma'_{ave} + 2S_u) \tag{1}$$

Where, σ'_{ave} is the average vertical effective stress and S_u is the undrained shear strength.

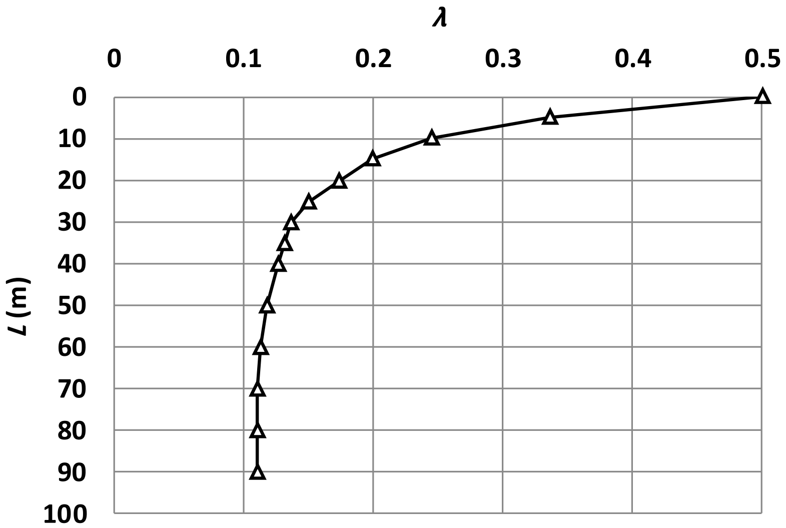

Figure 2: Relationship between the λ factor and the embedment depth of the pile (data is from Das (2011))

2- Alpha (α) method:

This method proposes that the skin friction of a driven pile is a percentage of the undrained shear strength by using an empirical adhesion factor called α as shown in Equation 2. This α empirical factor was originally proposed by Tomlinson in 1957 (Terzaghi, 1996). However, there are three methods currently available to estimate the α factor. These methods can be summarized as follows:

- Sladen (1992) method:

Sladen (1992) proposed Equation 3 to predict the α coefficient. The C factor in Equation 3 is equal to or greater than 0.5 for driven piles (Das, 2011).

- ISO (2016) method:

ISO (2016) suggested two different equations to calculate the α factor depending on the ratio of the undrained shear strength to the average vertical effective stress as shown in Equations 4 and 5.

- Terzaghi et al. (1996) method:

Terzaghi et al. (1996) suggested predicting the α coefficient from Figure 3; Pa in Figure 3 is the atmospheric pressure (100 kPa). This Figure has been developed based on data collected from Dennis and Olson (1983) and Stas and Kulhawy (1984). However, Terzaghi et al. (1996) also recommended multiplying the α coefficient obtained from Figure 3 by 0.54 (i.e. a reduction factor) for piles with a length equal to or greater than 50 m. Also, for pile lengths from 30 m to 50 m, the reduction factor varies linearly between 1.00 and 0.56.

$$fs = \alpha S_u \quad (2)$$

$$\alpha = C(\frac{\sigma'_{ave}}{S_u})^{0.45} \quad (3)$$

$$\alpha = 0.5(\frac{S_u}{\sigma'_{ave}})^{-0.5} \quad \text{for } \frac{S_u}{\sigma'_{ave}} \leq 1 \quad (4)$$

$$\alpha = 0.5(\frac{S_u}{\sigma'_{ave}})^{-0.25} \quad \text{for } \frac{S_u}{\sigma'_{ave}} > 1 \quad (5)$$

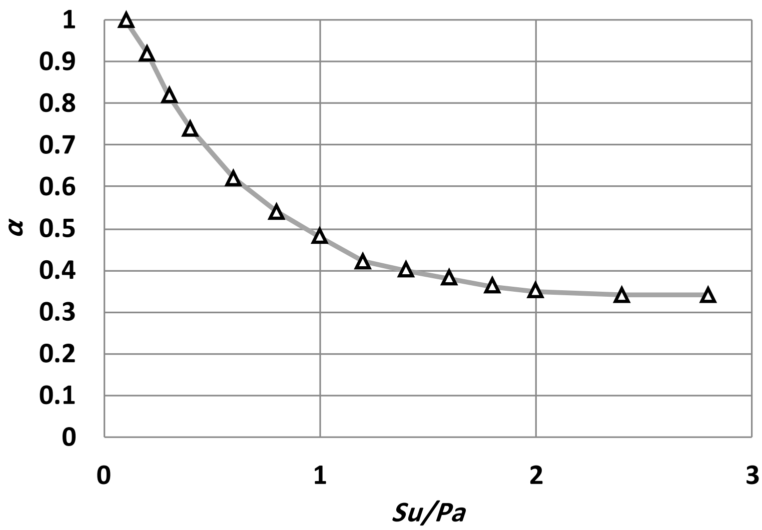

Figure 3: The α factor based on Terzaghi et al. (1996)

3- Beta (β) method

This method considers a different approach compared to the other two methods. In this method, the skin friction is determined using the drained angle of internal friction of the remolded clay ($ø'$) as shown in Equations 6 to 9 (Das, 2011). The beta factor ranges between 0.25 to 0.4 (Goh, 1995).

$$fs = \beta \sigma'_{ave} \tag{6}$$

$$\beta = K \ \tan ø' \tag{7}$$

$$K = 1 - \sin ø' \ \text{ for normally consolidated clay} \tag{8}$$

$$K = (1 - \sin ø')\sqrt{OCR} \text{ for over consolidated clay} \tag{9}$$

Where, OCR is the over-consolidation ratio.

3. Data used in the analyses

The data used in the current study have been adapted from a database of skin friction capacities of driven piles presented by Goh (1995). The database comprises 65 points of data on the skin friction capacity of driven piles (fs). In addition, the data contains the length of the pile (L), the diameter of the pile (D), the average vertical effective stress (σ'_{ave}) and the average undrained shear strength (S_u). Goh (1995) developed this database by collecting results from the literature; these results were for pile load tests conducted on timber and steel pipe piles. It is worth mentioning that these parameters have been selected as they are the most influential parameters with respect to the skin friction capacity of the pile. These parameters have also been used in previous studies for the prediction of the skin friction capacity of piles (Goh, 1995, Samui, 2008, 2011, 2019, Suman et al., 2016, Prayogo, 2018, Moayedi and Hayati, 2018b).

Table 2 shows the mean, standard deviation, maximum value (Max.), minimum value (Min.) and range of the collected data.

Table 2: Statistics of the data used in this study

Statistic indicator	Parameter				
	L (m)	D (cm)	σ'_{ave} (kPa)	S_u (kPa)	fs (kPa)
Mean	21.55	31.45	124.58	62.16	40.85
Standard deviation	16.37	16.61	127.71	60.03	36.52
Max.	96.00	76.70	718.00	335.00	192.10
Min.	4.60	11.40	19.00	9.00	8.00
Range	91.40	65.30	699.00	326.00	184.10

4. Multi-objective evolutionary polynomial regressions analysis (EPR)

Multi-Objective Evolutionary Polynomial Regression (MOGA-EPR) is a genetic algorithm-based regression analysis developed by Giustolisi and Savic (2009) based on the original evolutionary polynomial regression analysis developed by Giustolisi and Savic (2006). The methodology of MOGA-EPR is based on using a genetic algorithm in combination with a regression analysis (Alzabeebee et al., 2018, 2019; Alzabeebee, 2019, 2020). In this method, the 'fitting' is conducted utilizing the least square method and the selection of the best fitting model is done using the genetic algorithm. The MOGA-EPR controls the model fitness and model complexity using spread functions to enable more robust analyses (Giustolisi and Savic, 2009). This method also controls overfitting issues by using penalization procedures.

Equation 10 presents the starting point of the MOGA-EPR (Giustolisi and Savic, 2006). This equation produces an over-determined system, which is solved based on the least square methodology (Giustolisi and Savic, 2006).

$$y = \sum_{j=1}^{m} F\big(\mathrm{X}, f(\mathrm{X}), a_j\big) + a_0 \qquad (10)$$

Where y is the estimated output skin friction, a_j is a constant value, F is an assumed governing function between the input and the output variables; this function develops as the analysis time increases and based on artificial intelligence. X represents the independent variables matrix, f is the general form of the output function and m is the maximum number of terms in the produced equation and it is set by the user, and a_0 is the bias.

After solving Equation 10, the MOGA-EPR is formulated to find the model, which provides the best fit to the data by using different combinations of the exponents with the aid of artificial intelligence. Finally, the performance of the developed model is judged by determining a coefficient called the coefficient of determination (CD) and the model which scores the highest CD is selected; the CD is determined using Equation 11 (Alani et al., 2014a, b; Faramarzi et al., 2014). It is worth noting that the exponents considered in the EPR analysis are also controlled by the user. More information on the MOGA-EPR can be found in Alani et al. (2014); Faramarzi et al. (2014); Ahangar-Asr et al. (2014) and Alzabeebee (2017).

$$CD = 1 - \frac{\sum_N \left(fs_{(m)} - fs_{(p)}\right)^2}{\sum_N \left(fs_{(m)} - \frac{1}{N}\sum_N fs_{(p)}\right)^2} \tag{11}$$

Where, $fs_{(m)}$ is the measured skin friction, $fs_{(p)}$ is the predicted skin friction, and N is the number of the input data used in the development of the model.

5. Criteria considered to evaluate the accuracy of the MOGA-EPR model and the analytical methods

The quality of the prediction of the MOGA-EPR model and the available analytical methods have been assessed following a statistical based methodology similar to previous studies (Ozer et al., 2008; Alkroosh et al., 2014, 2015; Onyejekwe et al., 2015; Huang et al., 2019). The following points summarize the statistical measures used in the evaluation methodology:

1- The first statistical measure was based on finding the error in the prediction by calculating the mean absolute error (MAE) and the root mean square error (RMSE). Equations 12 and 13 show the mathematical formulation of the MAE and the RMSE (Ozer et al., 2008; Onyejekwe et al., 2015; Huang et al., 2019). The lower the MAE and the RMSE, the better the prediction. It is worth mentioning that the MAE has been considered because it provides insight into the average error of the prediction. In addition, the RMSE has been considered because it provides useful insight into the large error of the prediction, as the errors are squared before they are averaged as can be clearly noted in Equation 13 (Ashtiani et al., 2018).

$$MAE = \frac{1}{n}\sum_{1}^{n}\left|fs_{(p)} - fs_{(m)}\right| \tag{12}$$

$$RMSE = \sqrt{\frac{1}{n}\sum_{1}^{n}\left(fs_{(p)} - fs_{(m)}\right)^{2}} \tag{13}$$

Where, n is the number of data points used in the evaluation; $fs_{(p)}$ is the predicted skin friction of the pile; and $fs_{(m)}$: is the skin friction measured in the field.

2- The second statistical measure was based on calculating the mean (μ) of the ratio of the predicted skin friction to the measured skin friction as shown in Equation 14 (Onyejekwe et al., 2015). The expected range of the mean is zero to infinity. However, the optimum prediction should score a mean equal to 1 (Onyejekwe et al., 2015). The predictive model underestimates the skin friction if the mean is less than one and overestimates the skin friction if the mean is higher than one.

$$\mu = \frac{1}{n}\sum_{1}^{n}\left(\frac{fs_{(p)}}{fs_{(m)}}\right) \tag{14}$$

3- The third statistical measure was the standard deviation (σ) of the predicted skin friction to the measured skin friction. The standard deviation is calculated using Equation 15. The standard deviation provides a good indication to the distribution of the predicted values around the mean. The range of the standard deviation is between zero and one. A zero value provides the optimum prediction in which the scatter of the prediction around the mean a minimum. However, a value of one means a maximum scatter around the mean. Hence, the closer the standard deviation is to zero, the better the prediction (Alkroosh and Nikraz, 2014).

$$\sigma = \sqrt{\frac{\sum_{1}^{n}\left(\frac{fs_{(p)}}{fs_{(m)}} - \mu\right)^{2}}{n-1}} \tag{15}$$

4- The fourth statistical measure was the coefficient of determination (R^2). The R^2 measures the average error of the prediction. The R^2 ranges between zero and one, with an optimum value of one. Hence, the closer R^2 is to one, the better the prediction accuracy (Alzabeebee et al. 2017; Tinoco et al. 2019). R^2 is calculated using Equation 16 (Mohammadzadeh et al., 2019).

$$R^2 = \frac{\sum_{i=1}^{n}({fs_{(p)}}_i - {fs_{(p)}}_{average})({fs_{(m)}}_i - {fs_{(m)}}_{average})}{\sqrt{\sum_{i=1}^{n}({fs_{(p)}}_i - {fs_{(p)}}_{average})^2 \sum_{i=1}^{n}({fs_{(m)}}_i - {fs_{(m)}}_{average})^2}} \tag{16}$$

Where, ${fs_{(p)}}_{average}$ is the average of the predicted skin friction values and ${fs_{(m)}}_{average}$ is the average of the measured skin friction values.

5- The fifth statistical measure was the variance account for (VAF). The VAF is usually employed to check the correctness of the predictive model. This is done by comparing the measured and the predicted output using Equation 17 (Armaghani et al., 2017). A VAF value of 100 means that the predictive model provides a perfect estimation of the output. Therefore, the closer the VAF of the predictive model to 100, the better the prediction (i.e. lower variance).

$$VAF = \left[1 - \frac{var(fs_{(m)} - fs_{(p)})}{var(fs_{(m)})}\right] \times 100 \tag{17}$$

6- The final statistical measure was the $a20 - index$. This statistical measure evaluates the percentage of the predictive outputs that falls within the range of 80% to 120% of the measured output. A value of the $a20 - index$ of 1.0 means that the predictions of the models are equal to, or below, a 20% error. In addition, the closer the $a20 - index$ is to 1 the better, as it means that there are many predictions that are equal to, or below, a 20% error. The $a20 - index$ is calculated using Equation 18 (Armaghani, 2020).

$$a20 - index = \frac{m20}{n} \quad (18)$$

Where, $m20$ is the number of results where the predicted to the measured skin friction is between 0.8 to 1.2.

6. Development of the MOGA-EPR model

The data, with statistics shown in Table 2, has been used to develop the MOGA-EPR model. This data has been divided into two groups: training data and testing data. 80% of the data has been used in the model development (training stage) and 20% of the data has been used in the model testing and validation (testing stage). It should be noted that dividing the data into training and test data is common in the development of data driven models, i.e. the training data is used in the training and the development of the MOGA-EPR model, and the performance of the developed model has been checked using independent data that has not been used in the training stage. Hence, the use of testing data ensures the robustness and accuracy of the developed model (Alani et al., 2014a, b; Faramarzi et al., 2014; Ahangar-Asr et al., 2014; Alzabeebee, 2017, 2019, 2020; Alzabeebee et al., 2018, 2019). However, to avoid model extrapolation the variables of the testing data should be in the range of the data used in the model training (i.e. model development) (Alzabeebee, 2017, 2019, 2020; Alzabeebee et al., 2018, 2019). Hence, the data have been randomly shuffled and divided into two group, then statistical analyses have been conducted to ensure that the training and testing data are consistent. Tables 3 and 4 show the mean, standard deviation, maximum value (Max.), minimum value (Min.) and the range of both the training and testing data, respectively. The tables demonstrate the consistency of the training and the validation data.

The MOGA-EPR analysis was conducted after ensuring that the data are consistent. Several structures and exponents of the mathematical model are now examined, and the performance of the obtained model is also studied using the criteria discussed previously in this paper. Equation 18 shows the best mathematical model obtained from the MOGA-EPR analysis. Figures 4a, b, c, d, e, f and g show the obtained MAE, $RMSE$, μ, σ, R^2, VAF and $a20 - index$ values for the training and testing data, respectively. Figure 4a clearly shows that the developed MOGA-EPR model gives a very good accuracy with a MAE of 3.4 and 4.2 for the training and testing data, respectively. The obtained $RMSE$ results presented in Figure 4b also show that the model offers a very good prediction, where the $RMSE$ is equal to 4.6 and 5.3 for the training and testing data, respectively. The μ values shown in Figure 4c give additional proof of the accuracy, where the developed model slightly overestimates the skin friction as the obtained μ values are 1.03 and 1.12 for the training and testing data, respectively. Furthermore, the obtained values of the σ (Figure 4d) and R^2 (Figure 4e) also show the strength of the model, where σ is equal to 0.24 for the training and 0.15 for the testing data and R^2 is very close to one being equal to 0.98 and 0.91 for the training and the testing data, respectively. The results of the VAF (Figure 4f) provides additional trust in the robustness of the model as the obtained VAF is very close to 100 for training and testing data (99 for training data and 97 for testing data). The $a20-index$ analyses (Figure 4g) also demonstrate the prediction capabilities of the models as the percentage of the obtained predictions with error less than or equal to 20% is 75% and 77% for training and testing data, respectively.

$$fs = 28.44\frac{D.\sqrt{S_u}}{L^3} - 3\times10^{-7}\frac{\sqrt{D}.\sqrt{\sigma'_{ave}}.{S_u}^3}{L^2} - 83.81\frac{\sqrt{D}}{\sqrt{L}.\sqrt{\sigma'_{ave}}} + 0.023\frac{\sqrt{D}.\sqrt{\sigma'_{ave}}.S_u}{\sqrt{L}} + 27.17 \qquad (18)$$

Figures 5a and b show the relationship between the predicted and measured skin friction values. It is clear from the figures that most of the points are on or very close to the no-error line, which means that the developed model provides very good prediction and providing further confidence in the developed MOGA-EPR model.

430 Table 3: Statistics of the training data used in the MOGA-EPR analysis

Statistical indicator	Parameter				
	L (m)	D (cm)	σ'_{ave} (kPa)	S_u (kPa)	fs (kPa)
Mean	20.56	30.80	119.57	63.13	41.80
Standard deviation	16.44	17.12	132.08	63.65	38.38
Max.	96.00	76.70	718.00	335.00	192.10
Min.	4.60	11.40	19.00	9.00	8.00
Range	91.40	65.30	699.00	326.00	184.10

431

432

433 Table 4: Statistics of the testing data used in the MOGA-EPR analysis

Statistical indicator	Parameter				
	L (m)	D (cm)	σ'_{ave} (kPa)	S_u (kPa)	fs (kPa)
Mean	25.52	34.05	144.62	58.31	37.03
Standard deviation	16.08	14.69	110.94	44.50	28.83
Max.	66.40	61.00	448.00	185.00	109.20
Min.	9.40	15.00	49.00	17.00	12.00
Range	57.00	46.00	399.00	168.00	97.20

434

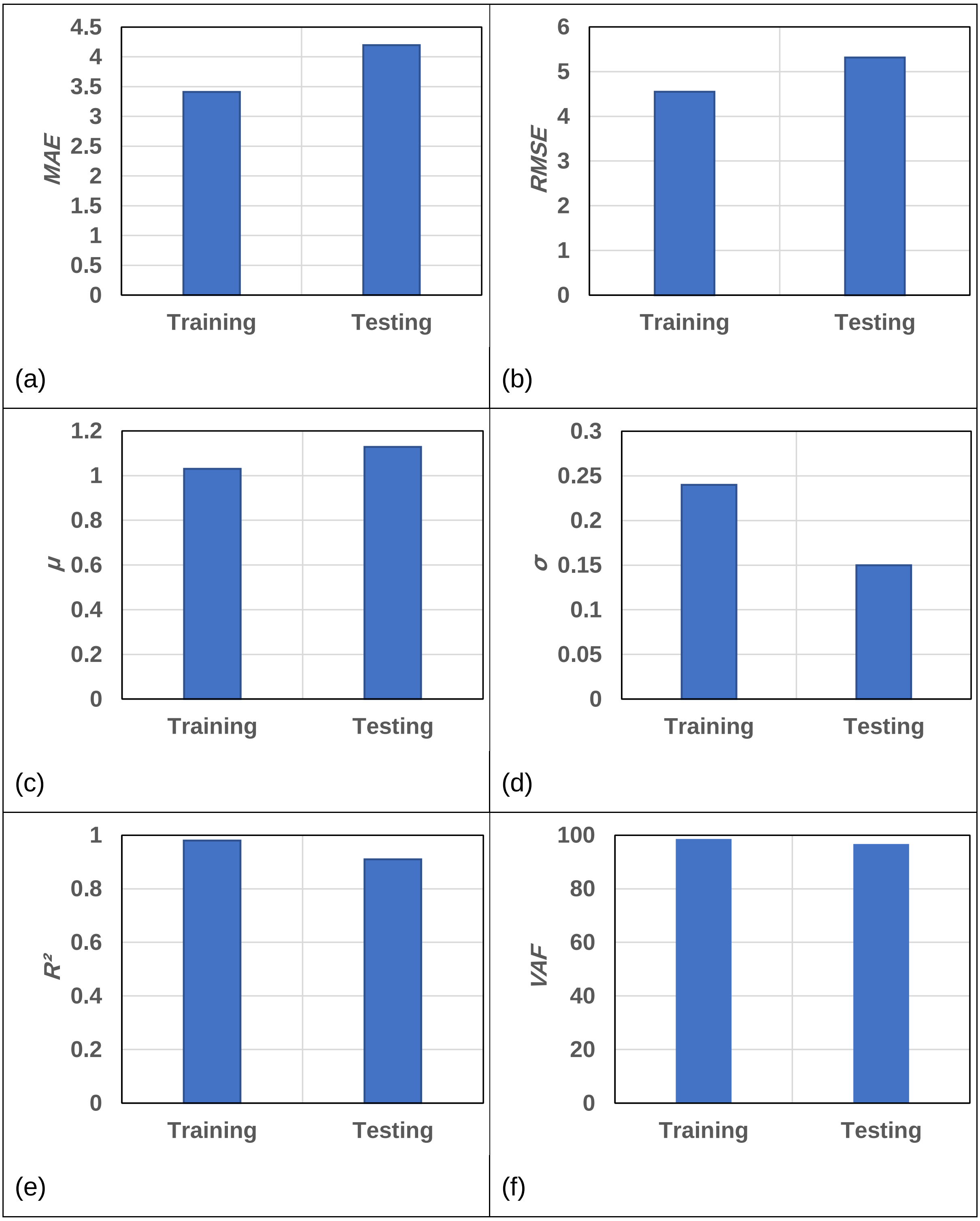

4.5
4
3.5
3
2.5
2
1.5
1
0.5
0
MAE
Training
Testing
(a)
6
5
4
3
2
1
0
RMSE
Training
Testing
(b)
1.2
1
0.8
0.6
0.4
0.2
0
μ
Training
Testing
(c)
0.3
0.25
0.2
0.15
0.1
0.05
0
σ
Training
Testing
(d)
1
0.8
0.6
0.4
0.2
0
R²
Training
Testing
(e)
100
80
60
40
20
0
VAF
Training
Testing
(f)

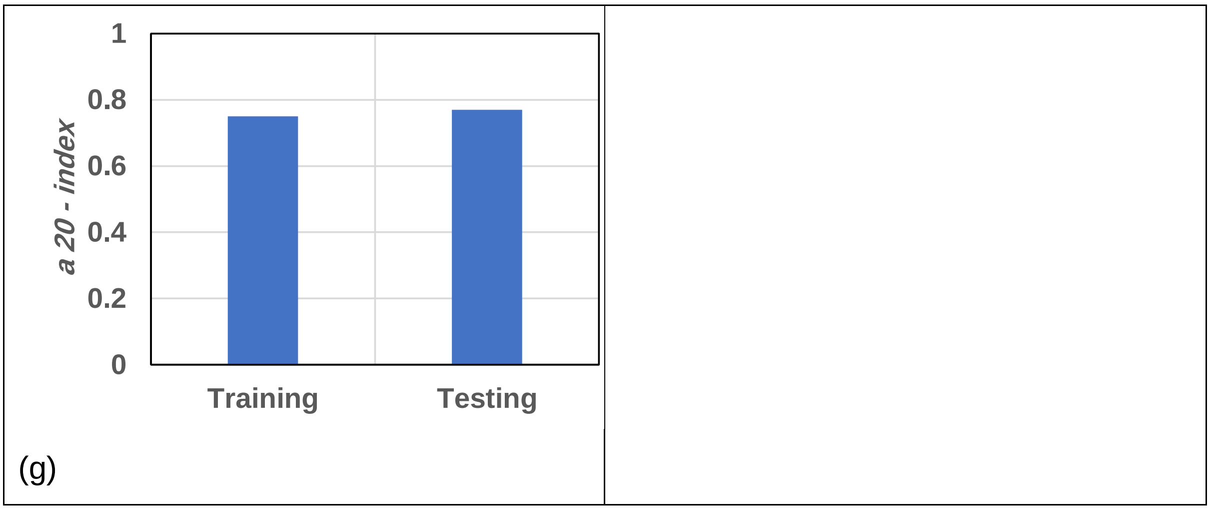

Figure 4: Results of the statistical analyses of the MOGA-EPR model: (a) Mean absolute error (MAE); (b) root mean square error ($RMSE$); (c) Mean (μ); (d) standard deviation (σ); (e) coefficient of determination (R^2); (f) variance account for (VAF); and (g) $a20 - index$

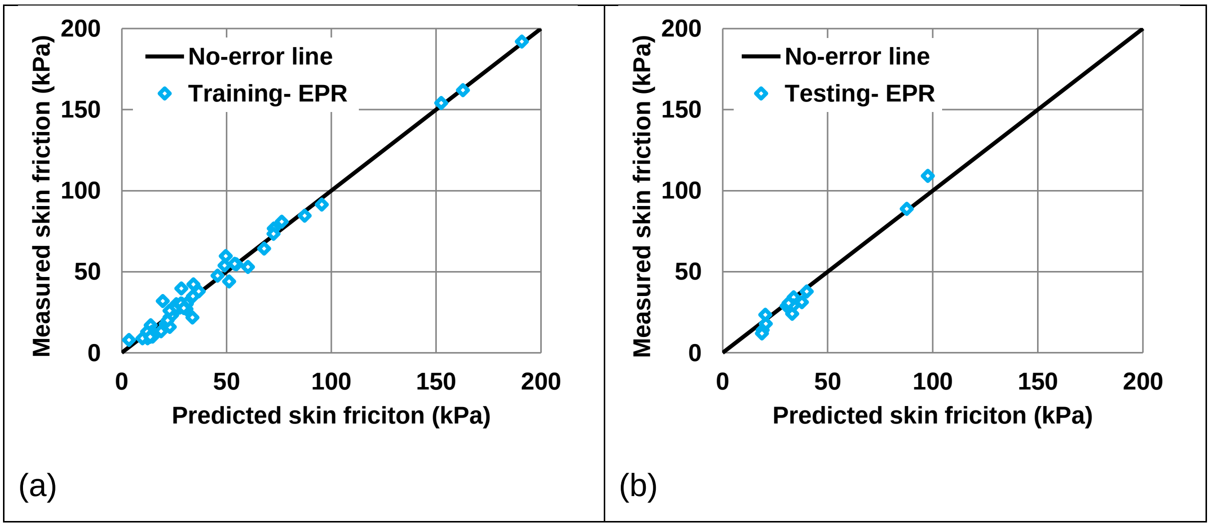

Figure 5: Relationship between the MOGA-EPR predicted skin friction and measured skin friction for: (a) training data; and (b) testing data

7. Evaluation of the accuracy of the analytical methods

It is very important to understand the limitations and the accuracy of the current analytical methods. Thus, the accuracy of the previously discussed analytical methods has been assessed in this section using the assessment methodology discussed earlier in this paper. The results of the assessment have also been compared with the MOGA-EPR model. The β factor has been considered equal to 0.33 in the calculation of the skin friction capacity using the Beta method; this value is the average of the expected range for the β factor (Goh, 1995). Furthermore, the three methods mentioned previously to calculate the α factor have been considered in this assessment; the Sladen (1992) method has been named Alpha 1, the ISO method has been named Alpha 2, and the Terzaghi et al. method has been named Alpha 3.

Figures 6a, b, c, d, e, f and g show the obtained MAE, $RMSE$, μ, σ, R^2, VAF and $a20-index$ for all of the analytical methods, respectively. In addition, Figures 7a, b, c, d and e show the relationship of the predicted and measured skin friction for all of the analytical methods. Comparing Figures 6 and 7 with Figures 4 and 5 clearly shows the MOGA-EPR model predicts the skin friction capacity better than all of the other analytical methods. Furthermore, Figure 6 shows that the Lambda method predicted the skin friction with lowest error (Figures 6a and b), lowest standard deviation (Figure 6d), highest coefficient of determination (Figure 6e), highest value for the variance account for (Figure 6f) compared with the Alpha and Beta methods. However, the mean (μ) of the Lambda method was relatively higher than the other methods (Figure 6c). Furthermore, the results of the mean (μ) show that, on average, all the analytical methods tend to overestimate the skin friction of the pile except for the Alpha 3 method which, on average, slightly underestimates the skin friction capacity. In addition, Figure 6g reveals that on average the Lambda, Alpha 1 and Alpha 2 methods produces similar accuracy in terms of the percentage of the predictions with error equal to or lower than 20%, where the scored $a20-index$ value is equal to 0.60, 0.62 and 0.63 for Lambda, Alpha 1 and Alpha 2 methods, respectively. Figures 7a, b, c, d and e show that Lambda method provides less scatter around the mean compared with the Alpha and Beta methods and this is confirmed by the obtained coefficient of determination and VAF, which is higher for the Lambda method as shown in Figures 6e and f.

It is also obvious from Figure 6 that the Alpha 1 and Alpha 2 methods predict the skin friction capacity with slightly higher MAE (8.9 for Alpha 1 and 8.1 for Alpha 2), $RMSE$ (14.4 for Alpha 1 and 13.0 for Alpha 2) and σ (0.32 for Alpha 1 and 0.27 for Alpha 2) compared than the Lambda method. In addition, the Alpha 1 and Alpha 2 methods predict the skin friction capacity with slightly lower R^2 (0.85 for Alpha 1 and 0.88 for

Alpha 2) and VAF (85 for Alpha 1 and 88 for Alpha 2) than the Lambda method. The Alpha 1 and Alpha 2 methods also achieved a μ value closer to 1 ($\mu = 1.02$ for the Alpha 1 method and $\mu = 1.07$ for the Alpha 2 method) compared with the Lambda method ($\mu = 1.16$). Thus, the Alpha 1 and Alpha 2 methods can be both ranked second compared with other analytical methods.

Finally, Figures 6 and 7 also show that the Beta method is the worst performing method and the error produced using this method is very high ($MAE = 17.2$ and $RMSE = 28.0$) compared with other methods. Also, the σ value obtained using the Beta method is 1.00; this means a maximum scatter around the mean and can also be confirmed by the very low coefficient of determination calculated using this method, which is equal to 0.55 (Figure 6e) and the very low VAF, which is equal to 40 (Figure 6f). The very low coefficient of determination of the Beta method can also be evidenced by Figure 7e, which shows a large scatter of the predicted-measured relationship compared with the no-error line. Also, the $a20 - index$ for the Beta method is very low and is equal to 0.37; this means only 37% of the predictions are with error equal to or less than 20%. Hence, the Beta method ranked last based on this assessment.

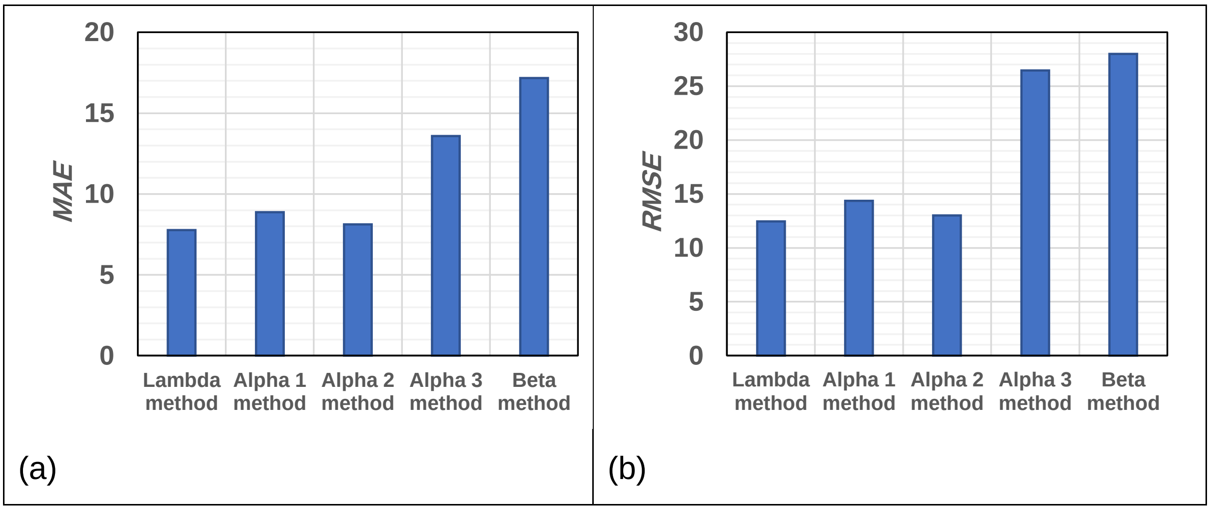

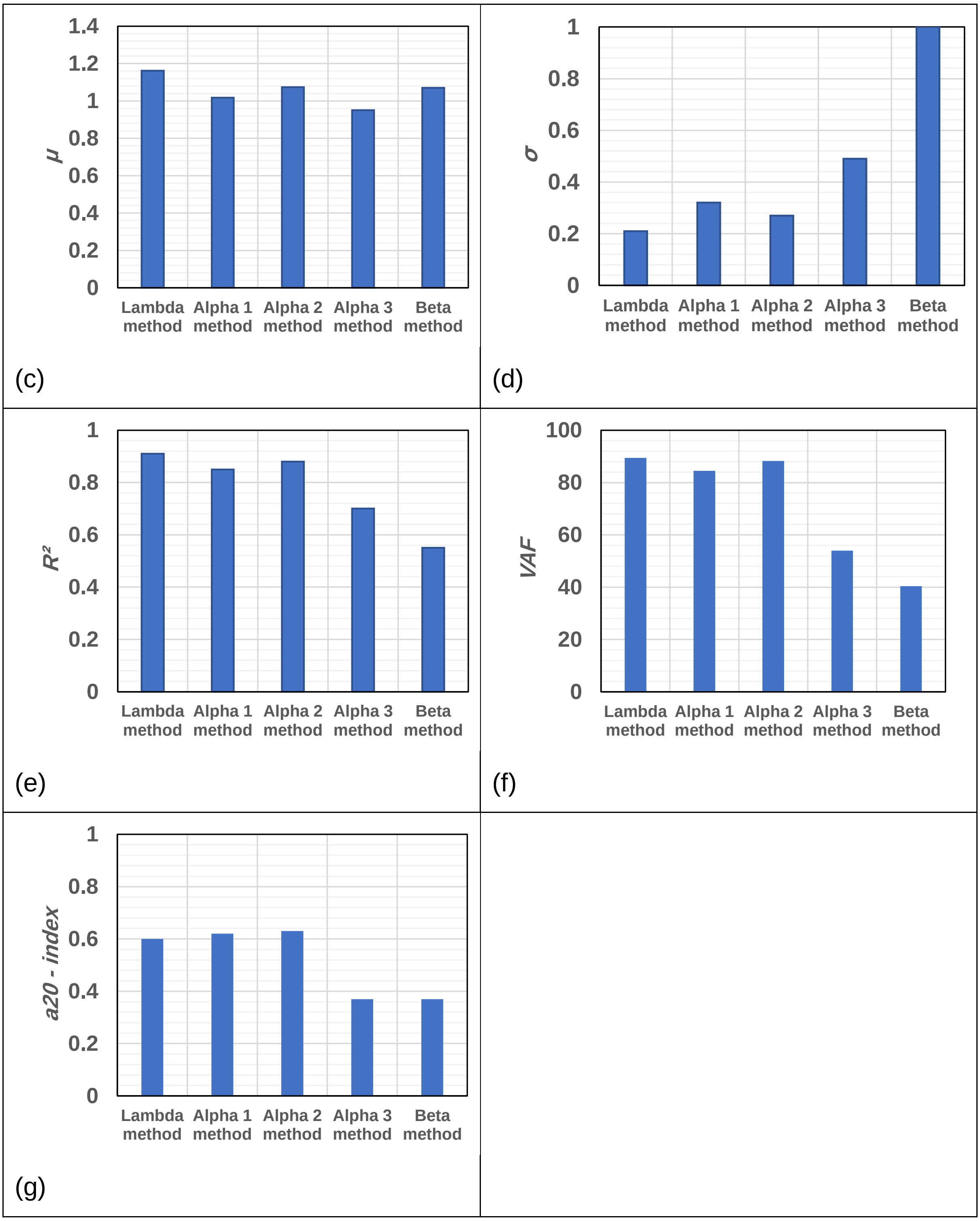

Figure 6: Results of the statistical analysis: (a) Mean absolute error (MAE); (b) root mean square error ($RMSE$); (c) Mean (μ); (d) standard deviation (σ); and (e) coefficient of determination (R^2); (f) Variance account for (VAF); and (g) $a20 - index$

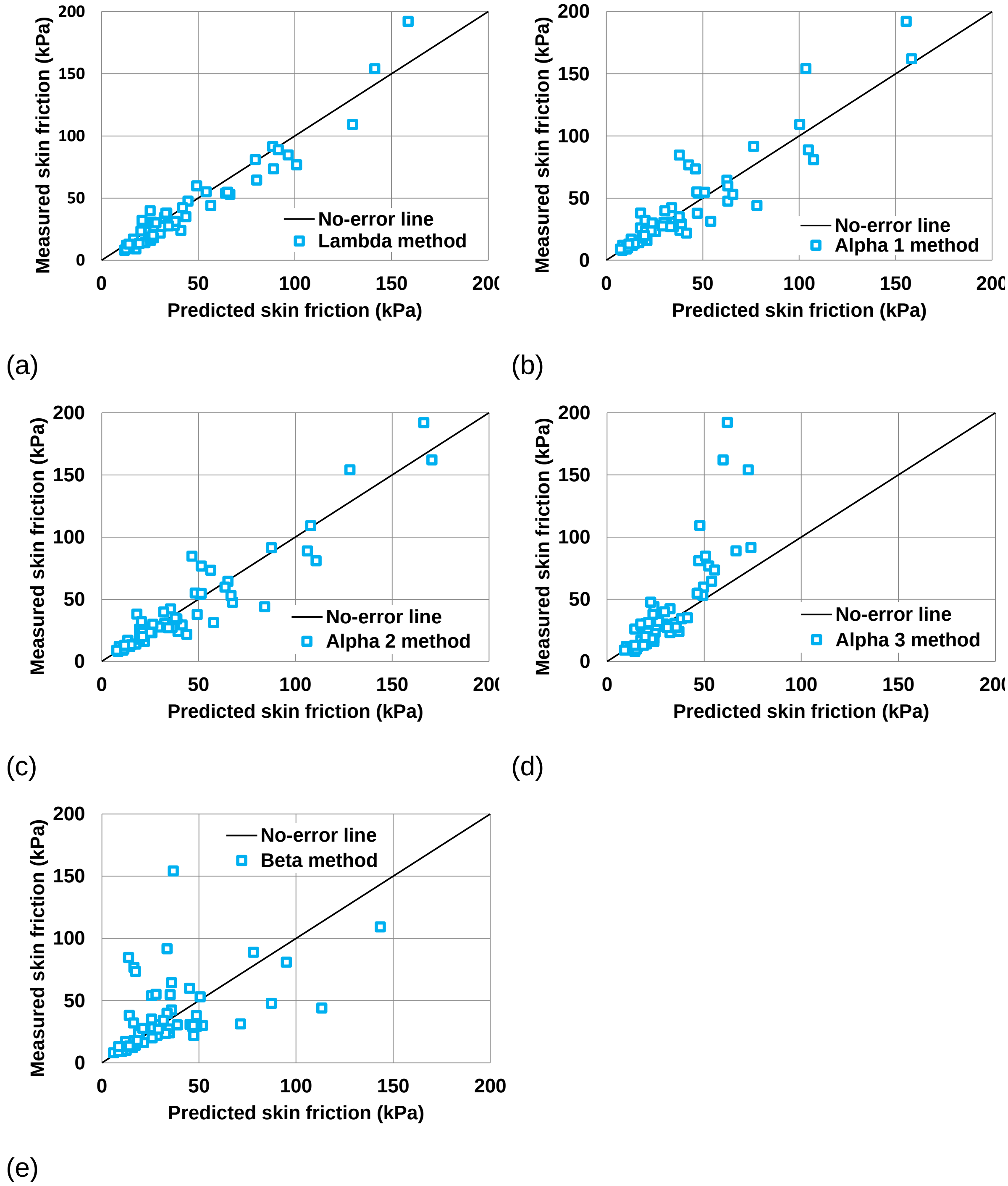

Figure 7: Predicted versus measured skin friction using: (a) Lambda method; (b) Alpha 1 method; (c) Alpha 2 method; (d) Alpha 3 method; and (e) Beta method

8. Conclusions

The results of this study have demonstrated the abilities of the multi-objective evolutionary (MOGA-EPR) polynomial regression analysis in predicting the skin friction capacity of driven piles embedded in clay. The MOGA-EPR model achieved a very low error, a mean value close to 1, low standard deviation, very high coefficient of determination, very high value for the variance account for and high value for the $a20 - index$ for both training and testing data. Furthermore, the accuracy of the MOGA-EPR model has been confirmed by presenting the relationship between the predicted and measured skin friction values for both the training and testing data and the presented relationships demonstrated the accuracy of the MOGA-EPR model as most of the points were on or very close to the no-error line for both the testing and training data. In addition, the MOGA-EPR model has been compared with the available analytical methods in the literature and the results have demonstrated that the developed model is better than the available analytical methods as the MOGA-EPR model performed better based on the statistical measures. Thus, the developed model can be used with confidence in future designs. However, it is worth stating that the developed model has been trained and tested based on lengths of pile ranging from 4.60 m to 96.00 m, diameters of piles ranging from 11.40 cm to 76.70 cm and undrained cohesion ranging from 9.00 kPa to 355 kPa. Hence, the model should be used for designs within these ranges. Nonetheless, the developed model can also be tested further in the future when new data becomes available.

In addition, assessing the available analytical methods showed that the Lambda method is the most accurate method compared with Alpha and Beta methods. This method scored an mean absolute error (MAE) of 7.8, a root mean square error ($RMSE$) of 12.5, a mean (μ) of 1.16, a standard deviation (σ) of 0.21, a coefficient of determination (R^2) of 0.91, a value for the variance account for (VAF) of 89 and $a20 - index$ of 0.6. Hence, this method can also be used as an alternative to the MOGA-EPR model developed in this study. Furthermore, the Alpha 1 method (Sladen, 1992) and Alpha 2 method (ISO, 2016) also scored low errors and high coefficient of determination; the errors of both methods are slightly higher than the Lambda method. The Alpha 1 and Alpha 2 methods also scored a μ closer to 1 than the Lambda method; therefore, both methods can be ranked second. The Beta method scored lowest compared with the other analytical methods with a MAE of 17.2, a $RMSE$ of 28.0, a μ of 1.07, a σ of 1.00, a R^2 of 0.55, a VAF of 40 and $a20 - index$ of 0.37. The developed mathematical model in this paper and the results of the assessment of the analytical methods are very useful to geotechnical engineers and will help to achieve better pile designs in the future.

References

Ahangar-Asr, A. and Javadi, A.A., 2016. Air losses in compressed air tunneling: a prediction model. Proceedings of the ICE-Engineering and Computational Mechanics, 169(3), pp.140-147.

Ahangar-Asr, A., Faramarzi, A. and Javadi, A.A., 2018. An evolutionary modelling approach to predicting stress-strain behaviour of saturated granular soils. Engineering Computations, 35(8), pp.2931-2952.

Ahangar-Asr, A., Javadi, A.A., Johari, A. and Chen, Y., 2014. Lateral load bearing capacity modelling of piles in cohesive soils in undrained conditions: an intelligent evolutionary approach. Applied Soft Computing, 24, pp.822-828.

Alani, A.M. and Faramarzi, A., 2014b. An evolutionary approach to modelling concrete degradation due to sulphuric acid attack. Applied Soft Computing, 24, pp.985-993.

Alani, A.M., Faramarzi, A., Mahmoodian, M. and Tee, K.F., 2014a. Prediction of sulphide build-up in filled sewer pipes. Environmental technology, 35(14), pp.1721-1728.

Alavi, A.H. and Sadrossadat, E., 2016. New design equations for estimation of ultimate bearing capacity of shallow foundations resting on rock masses. Geoscience Frontiers, 7(1), pp.91-99.

Alkroosh, I. and Nikraz, H., 2011a. Correlation of pile axial capacity and CPT data using gene expression programming. Geotechnical and Geological Engineering, 29(5), pp.725-748.

Alkroosh, I. and Nikraz, H., 2011b. Simulating pile load-settlement behavior from CPT data using intelligent computing. Central European Journal of Engineering, 1(3), pp.295-305.

Alkroosh, I. and Nikraz, H., 2012. Predicting axial capacity of driven piles in cohesive soils using intelligent computing. Engineering Applications of Artificial Intelligence, 25(3), pp.618-627.

Alkroosh, I. and Nikraz, H., 2014. Predicting pile dynamic capacity via application of an evolutionary algorithm. Soils and Foundations, 54(2), pp.233-242.

Alkroosh, I.S., Bahadori, M., Nikraz, H. and Bahadori, A., 2015. Regressive approach for predicting bearing capacity of bored piles from cone penetration test data. Journal of Rock Mechanics and Geotechnical Engineering, 7(5), pp.584-592.

Alzabeebee, S., 2017. Enhanced design approaches for rigid and flexible buried pipes using advanced numerical modelling. PhD Thesis, University of Birmingham, United Kingdom.

Alzabeebee, S., 2019. Seismic response and design of buried concrete pipes subjected to soil loads. Tunnelling and Underground Space Technology, 93, p.103084.

Alzabeebee, S., 2020. Dynamic response and design of a skirted foundation subjected to vertical vibration. Geomechanics and Engineering, 20(4), pp. 345-358.

Alzabeebee, S., Chapman, D., Jefferson, I. and Faramarzi, A., 2017. The response of buried pipes to UK standard traffic loading. Proceedings of the Institution of Civil Engineers-Geotechnical Engineering, 170(1), pp.38-50.

Alzabeebee, S., Chapman, D.N. and Faramarzi, A., 2018. Development of a novel model to estimate bedding factors to ensure the economic and robust design of rigid pipes under soil loads. Tunnelling and Underground Space Technology, 71, pp.567-578.

Alzabeebee, S., Chapman, D.N. and Faramarzi, A., 2019. Economical design of buried concrete pipes subjected to UK standard traffic loading. Proceedings of the Institution of Civil Engineers-Structures and Buildings, 172(2), pp.141-156.

Armaghani, D.J., Asteris, P.G., Askarian, B., Hasanipanah, M., Tarinejad, R. and Huynh, V.V., 2020. Examining Hybrid and Single SVM Models with Different Kernels to Predict Rock Brittleness. Sustainability, 12(6), p.2229.

Armaghani, D.J., Mohamad, E.T., Narayanasamy, M.S., Narita, N. and Yagiz, S., 2017. Development of hybrid intelligent models for predicting TBM penetration rate in hard rock condition. Tunnelling and Underground Space Technology, 63, pp.29-43.

Armaghani, D.J., Raja, R.S.N.S.B., Faizi, K. and Rashid, A.S.A., 2017. Developing a hybrid PSO–ANN model for estimating the ultimate bearing capacity of rock-socketed piles. Neural Computing and Applications, 28(2), pp.391-405.

Ashtiani, R.S., Little, D.N. and Rashidi, M., 2018. Neural network based model for estimation of the level of anisotropy of unbound aggregate systems. Transportation Geotechnics, 15, pp.4-12.

Chen, W., Sarir, P., Bui, X.N., Nguyen, H., Tahir, M.M. and Armaghani, D.J., 2019. Neuro-genetic, neuro-imperialism and genetic programing models in predicting ultimate bearing capacity of pile. Engineering with Computers, DOI: https://doi.org/10.1007/s00366-019-00752-x.

Cherubini, C. and Vessia, G., 2007. Reliability approach for the side resistance of piles by means of the total stress analysis (α Method). Canadian Geotechnical Journal, 44(11), pp.1378-1390.

Das, B., 2011. Principles of Foundations Engineering, Seventh edition, Cengage Learning.

Dennis, N.D. and Olson, R.E., 1983. Axial capacity of steel pipe piles in clay. In From Soil Behavior Fundamentals to Innovations in Geotechnical Engineering: Honoring Roy E. Olson (pp. 176-194). ASCE.

Doherty, P. and Gavin, K., 2011. The shaft capacity of displacement piles in clay: a state of the art review. Geotechnical and Geological Engineering, 29(4), pp.389-410.

Faramarzi, A., 2011. Intelligent computational solutions for constitutive modelling of materials in finite element analysis. PhD. Thesis, University of Exeter, United Kingdom.

Faramarzi, A., Alani, A.M. and Javadi, A.A., 2014. An EPR-based self-learning approach to material modelling. Computers & Structures, 137, pp.63-71.

Fiore, A., Quaranta, G., Marano, G.C. and Monti, G., 2016. Evolutionary polynomial regression–based statistical determination of the shear capacity equation for reinforced concrete beams without stirrups. Journal of Computing in Civil Engineering, 30(1), p.04014111.

Giustolisi, O. and Savic, D.A., 2006. A symbolic data-driven technique based on evolutionary polynomial regression. Journal of Hydroinformatics, 8(3), pp.207-222.

Giustolisi, O. and Savic, D.A., 2009. Advances in data-driven analyses and modelling using EPR-MOGA. Journal of Hydroinformatics, 11(3-4), pp.225-236.

Goh, A.T.C., 1995. Empirical design in geotechnics using neural networks. Géotechnique, 45(4), pp.709-714.

Harandizadeh, H., Armaghani, D.J. and Khari, M., 2019. A new development of ANFIS–GMDH optimized by PSO to predict pile bearing capacity based on experimental datasets. Engineering with Computers, pp.1-16.

Harandizadeh, H., Toufigh, M.M. and Toufigh, V., 2018a. Application of improved ANFIS approaches to estimate bearing capacity of piles. Soft Computing, DOI: https://doi.org/10.1007/s00500-018-3517-y.

Harandizadeh, H., Toufigh, M.M. and Toufigh, V., 2018b. Different neural networks and modal tree method for predicting ultimate bearing capacity of piles. International Journal of Optimization in Civil Engineering, 8(2), pp.311-328.

Huang, C.F., Li, Q., Wu, S.C., Liu, Y. and Li, J.Y., 2019. Assessment of empirical equations of the compression index of muddy clay: sensitivity to geographic locality. Arabian Journal of Geosciences, 12(4), p.122.

International Organization for Standardization (ISO), 2016. Petroleum and natural gas industries-specific requirements for offshore structures. Part 4: geotechnical and foundation design considerations. ISO 19901-4:2016, Geneva, Switzerland.

Ismail, A. and Jeng, D.S., 2011. Modelling load–settlement behaviour of piles using high-order neural network (HON-PILE model). Engineering Applications of Artificial Intelligence, 24(5), pp.813-821.

Li, J., Wang, X., Guo, Y. and Yu, X.B., 2019. Vertical bearing capacity of the pile foundation with restriction plate via centrifuge modelling. Ocean Engineering, 181, pp.109-120.

Milad, F., Kamal, T., Nader, H. and Erman, O.E., 2015. New method for predicting the ultimate bearing capacity of driven piles by using Flap number. KSCE Journal of Civil Engineering, 19(3), pp.611-620.

Moayedi, H. and Armaghani, D.J., 2018. Optimizing an ANN model with ICA for estimating bearing capacity of driven pile in cohesionless soil. Engineering with Computers, 34(2), pp.347-356.

Moayedi, H. and Hayati, S., 2018a. Applicability of a CPT-based neural network solution in predicting load-settlement responses of bored pile. International Journal of Geomechanics, 18(6), p.06018009.

Moayedi, H. and Hayati, S., 2018b. Artificial intelligence design charts for predicting friction capacity of driven pile in clay. Neural Computing and Applications, DOI: https://doi.org/10.1007/s00521-018-3555-5.

Mohammadzadeh D.S., Kazemi S.F., Mosavi A., Nasseralshariati E. and Joseph H. M. Tah. J.H.M., 2019. Prediction of Compression Index of Fine-Grained Soils Using a Gene Expression Programming Model. Infrastructures, 4(2), 26.

Momeni, E., Nazir, R., Armaghani, D.J. and Maizir, H., 2014. Prediction of pile bearing capacity using a hybrid genetic algorithm-based ANN. Measurement, 57, pp.122-131.

Momeni, E., Nazir, R., Armaghani, D.J. and Maizir, H., 2015. Application of artificial neural network for predicting shaft and tip resistances of concrete piles. Earth Sciences Research Journal, 19(1), pp.85-93.

Nassr, A., Esmaeili-Falak, M., Katebi, H. and Javadi, A., 2018b. A new approach to modeling the behavior of frozen soils. Engineering Geology, 246, pp.82-90.

Nassr, A., Javadi, A. and Faramarzi, A., 2018a. Developing constitutive models from EPR-based self-learning finite element analysis. International Journal for Numerical and Analytical Methods in Geomechanics, 42(3), pp.401-417.

Nejad, F.P. and Jaksa, M.B., 2017. Load-settlement behavior modeling of single piles using artificial neural networks and CPT data. Computers and Geotechnics, 89, pp.9-21.

Onyejekwe, S., Kang, X. and Ge, L., 2015. Assessment of empirical equations for the compression index of fine-grained soils in Missouri. Bulletin of Engineering Geology and the Environment, 74(3), pp.705-716.

Ozer, M., Isik, N.S. and Orhan, M., 2008. Statistical and neural network assessment of the compression index of clay-bearing soils. Bulletin of Engineering Geology and the Environment, 67(4), pp.537-545.

Prayogo, D. and Susanto, Y.T.T., 2018. Optimizing the prediction accuracy of friction capacity of driven piles in cohesive soil using a novel self-tuning least squares support vector machine. Advances in Civil Engineering, 2018.

Samui, P., 2008. Prediction of friction capacity of driven piles in clay using the support vector machine. Canadian Geotechnical Journal, 45(2), pp.288-295.

Samui, P., 2011. Prediction of pile bearing capacity using support vector machine. International Journal of Geotechnical Engineering, 5(1), pp.95-102.

Samui, P., 2019. Determination of Friction Capacity of Driven Pile in Clay Using Gaussian Process Regression (GPR), and Minimax Probability Machine Regression (MPMR). Geotechnical and Geological Engineering, pp.1-5.

Shahin, M.A., 2010. Intelligent computing for modeling axial capacity of pile foundations. Canadian Geotechnical Journal, 47(2), pp.230-243.

Shahin, M.A., 2014a. Load–settlement modeling of axially loaded drilled shafts using CPT-based recurrent neural networks. International Journal of Geomechanics, 14(6), p.06014012.

Shahin, M.A., 2014b. Load–settlement modeling of axially loaded steel driven piles using CPT-based recurrent neural networks. Soils and Foundations, 54(3), pp.515-522.

Shahin, M.A., 2016. State-of-the-art review of some artificial intelligence applications in pile foundations. Geoscience Frontiers, 7(1), pp.33-44.

Shaik, S., Krishna, K.S.R., Abbas, M., Ahmed, M. and Mavaluru, D., 2018. Applying several soft computing techniques for prediction of bearing capacity of driven piles. Engineering with Computers, DOI: https://doi.org/10.1007/s00366-018-0674-7.

Singh, G. and Walia, B.S., 2017. Performance evaluation of nature-inspired algorithms for the design of bored pile foundation by artificial neural networks. Neural Computing and Applications, 28(1), pp.289-298.

Sladen, J.A., 1992. The adhesion factor: applications and limitations. Canadian Geotechnical Journal, 29(2), pp.322-326.

Sladen, J.A., 1992. The adhesion factor: applications and limitations. Canadian Geotechnical Journal, 29(2), pp.322-326.

Stas, C.V. and Kulhawy, F.H., 1984. Critical evaluation of design methods for foundations under axial uplift and compression loading. Report for EPRI, No. EL3771, Cornell University.

Suman, S., Das, S.K. and Mohanty, R., 2016. Prediction of friction capacity of driven piles in clay using artificial intelligence techniques. International Journal of Geotechnical Engineering, 10(5), pp.469-475.

Terzaghi, K., Peck, R.B. and Mesri, G., 1996. Soil mechanics in Engineering Practice. John Wiley & Sons.

Tinoco, J., Alberto, A., da Venda, P., Correia, A.G. and Lemos, L., 2019. A novel approach based on soft computing techniques for unconfined compression strength prediction of soil cement mixtures. Neural Computing and Applications, https://doi.org/10.1007/s00521-019-04399-z

Vijayvergiya, V. A. and Focht, J. A., Jr., 1972. A new way to predict capacity of piles in clays. Proceedings of the 4th Offshore Technology Conference, Houston 2, 865-874.